*Textures and Microstructures*, 1988, Vols. 8 & 9, pp. 619–635
Reprints available directly from the publisher
Photocopying permitted by license only

Printed in the United Kingdom

# Improvement of Yield Locus Calculation from Pole Figures of Zircaloy Tubes

K. H. MATUCHA and P. WINCIERZ
*Metall-Laboratorium der Metallgesellschaft AG, Frankfurt/M, FRG*

*(Received 25 September, 1987)*

Dedicated to the memory of Professor Günter Wassermann

Improvement of yield locus calculation, i.e. better fit with experimental results, was achieved for Zircaloy tubes with deformation and recrystallization textures in the following way: (1) Replacement of information from $\{10\bar{1}0\}$- and (0001)-pole figures by identification of preferred orientation parallel to the tube axis in combination with the basal pole density distribution in the plane between radial and tangential direction as a function of the tilt angle $\gamma_i$. (2) Calculation of those parts of the yield locus which are independent of mechanical twinning. For uniaxial tensile stress parallel to the tube axis the slope $m$ of the yield locus line for prismatic glide is given by $m_i = \cos^2 \gamma_i$. (3) Calculation of yield locus parts depending on mechanical twinning using experimentally well established ratios of critical resolved shear stresses for prismatic slip and several twinning systems.

Mechanical twinning on $\{11\bar{2}2\}$-planes was confirmed by texture analysis of plastically deformed tubes after yield locus investigation.

KEY WORDS: Zircaloy tubes, pole figures, yield loci, model calculations, glide, twinning.

## 1 INTRODUCTION

The classical way of describing textures from pole-figures is the replacement of the textured polycrystal by one or a few single crystals with best orientation fit. G. Wassermann used this method very successfully in his numerous contributions to the research on textures. Especially his fundamental results on the effect of mechanical twinning on texture formation of metals and alloys with hcp

**Table 1** Chemical composition of Zircaloy-2 and Zircaloy-4 (Mass-%), alloying elements (ASTM-B 353-64 T)

| | Sn | Fe | Cr | Ni |
|---|---|---|---|---|
| Zircaloy-2 | 1.20–1.70 | 0.07–0.20 | 0.05–0.15 | 0.03–0.08 |
| Zircaloy-4 | 1.20–1.70 | 0.18–0.24 | 0.07–0.13 | — |

resp. fcc crystal structure were based on this method (Schmid and Wassermann 1928, 1930, Wassermann 1963). Also for the calculation of mechanical anisotropy, especially elastic moduli and yield stresses this method was applied (Wassermann and Grewen 1962).

Zircaloy-2 resp. -4 (chemical composition see Table 1) which are used as fuel rod cladding material in water cooled nuclear reactors have a fine grained microstructure consisting of hcp matrix crystals and dispersoids of Cr and Fe bearing intermetallic compounds. These tubes show due to their production route marked anisotropy under two-axial stresses. Plane-stress measurements resulted in yield loci having different shapes compared with the v. Mises ellipse (Mehan 1981, Miller and Swota 1963, Dressler *et al.* 1972). Texture was found to be the primary cause for anisotropic elasticity and yielding (Dressler *et al.* 1972, Dressler *et al.* 1973, Dressler *et al.* 1974, Dressler and Matucha 1977).

Calculation of the elastic behaviour under plane-stress conditions using as input the single crystal replacement for the texture and the elastic coefficients of Zirconium lead to results in good agreement with the measured values (Dressler *et al.* 1973).

However, an attempt to calculate the yield loci of Zircaloy tubes from their texture in a similar way as it had proved successfully for fcc metals and alloys, ran into difficulties because mechanical twinning has to be considered in addition to slip as further crystallographic deformation mechanism active already at the onset of plastic flow. These problems could largely be overcome if, considering the unipolar deformation, the twin systems were formally treated as slip systems, and certain conditions appropriate to the experimental yield loci were assumed for the critical resolved shear sthresses (CRSS) of prismatic slip and twinning (Dressler *et al.* 1972, 1973).

First calculations were made for tubes of Zircaloy 4 with different deformation textures. These textures were characterized by a $[10\bar{1}0]$

direction being parallel to the tube axis (AD) in all cases. The difference caused by the manufacturing process manifested itself in the tilt angle $\gamma$ of the basal poles against the radial direction in the plane described by the tangential (TD) and radial (RD) direction. If, for calculation purposes, the textures were replaced by two single crystal orientations symmetrical to the radial direction, the result was a qualitatively good fit between calculated and experimental yield loci.

This fit was poorer whenever the replacement of the texture by two single crystal orientations resulted only in a rough approximation of the measured texture (Dressler *et al.* 1972, Dressler *et al.* 1973, Dressler and Matucha 1977).

This was true particularly for changes in the texture of cold-worked tubes caused by isochronous annealing (Matucha 1978). Then the deformation texture (Figure 1) developed into the recrystallization texture (Figure 2). The change in the basal pole tilt angle $\gamma$ (Figure 3) during this process was relatively slight. The yield loci calculated for single crystals with $\gamma = \pm 30°$ and $[10\bar{1}0]$ parallel to AD or $\gamma = 0°$ and $[11\bar{2}0]$ parallel to AD exhibited a poorer qualitative fit to the measured yield loci than in the case of textures which could be better described by two single crystal orientations. On the basis of calculated yield surfaces of hcp single crystals Tomé and Kocks (1985) tried to calculate yield loci of cross-rolled and rolled Zircaloy-2. They replaced the texture of the materials by 17

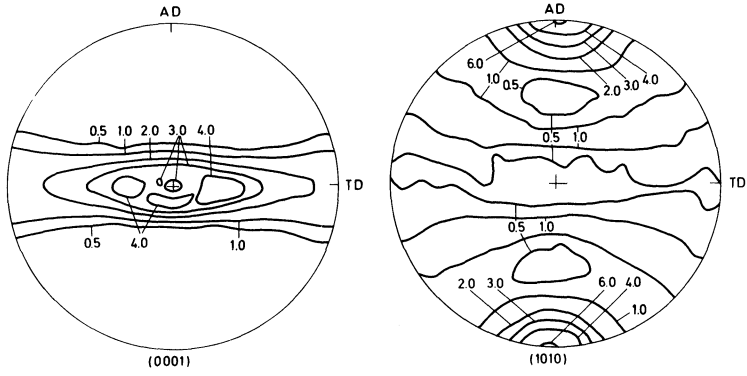


**Figure 1** Quantitative (0001)- and $\{10\bar{1}0\}$-pole figures of cold deformed Zircaloy-2 tubes (from Matucha, 1978).

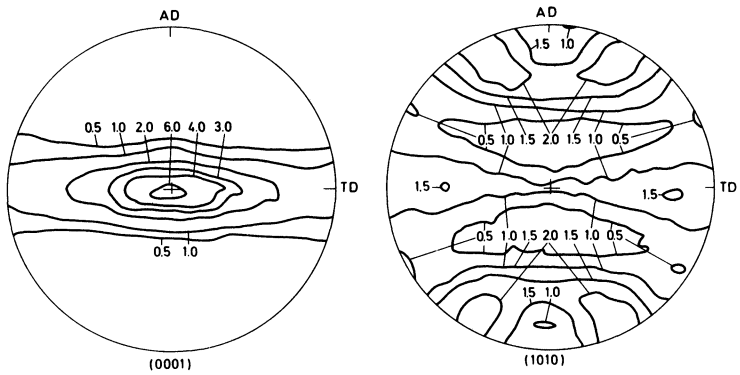


**Figure 2** Quantitative (0001)- and $\{10\bar{1}0\}$-pole figures of Zircaloy-2 tubes annealed 2 h at 750°C (from Matucha, 1978).

grains and considered prismatic slip and $\{10\bar{1}2\}$-twinning only. A reasonable fit with some measured points of the yield loci could be obtained, if for the rolled and cross-rolled Zircaloy-2 different ratios of the CRSS were used.

On the other hand yield loci for recrystallized Zircaloy tubes were calculated on the basis of ODF measurements and Taylor analyses (Spiegelberg and Anderson 1978) and then compared with some yield points that had been determined by experiments. However, even when the CRSS conditions were varied for slip and twinning, the fit between experimental and calculated yield points was only partly satisfactory.

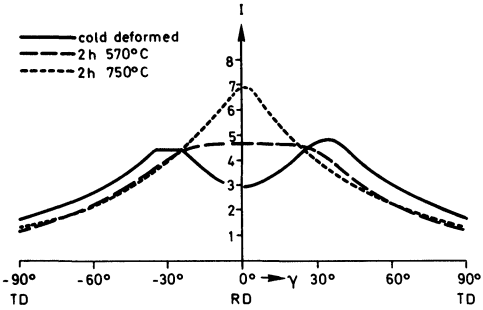


**Figure 3** Intensity of basal poles in the plane given by the radial and tangential directions of the tubes (from Matucha, 1978).

A semiempirical yield lines model for the yield locus of Zircaloy-4 tubes was proposed by Ciurchea (1985) using the $C_2^{00}$ coefficient found from the $\{10\bar{1}1\}$-pole figure. To fit the experimental yield loci of Dressler *et al.* (1972, 1973) specific rotation angles of the deformation systems, measured yield strengths in the axial and tangential directions and the $C_2^{00}$-coefficient of the cold worked specimen determined by Ciurchea (1985) were used. Due to the fit procedure the agreement of experimental and fitted data was good, although the real textures of the tubes were not taken into account.

The aim of the present investigation was to improve the agreement between measured and calculated yield loci using the classical single crystal replacement. As in the case of fcc metals with complex textures (Althoff and Wincierz 1972, Althoff 1973, Tilch *et al.* 1982) a better fit should be achieved by using more single crystal orientations for the replacement.

The improvement of the calculated yield loci should relate to both types of yield locus segments: Those which do not depend on mechanical twinning and those which do. Further the occurrence of mechanical twinning under the predicted stress conditions had to be proven.

## 2 CALCULATION OF YIELD LOCI

### 2.1 Yield loci for single crystals

If tubes with deformation textures are replaced by tubular single crystals with $[10\bar{1}0]$ parallel to AD and a tilt angle $\gamma$ of the basal pole, the effective shear stresses $\sigma_{eg}$ for each crystallographic deformation system defined by a crystallographic plane $e$ and a direction $g$ can be calculated as a function of the applied stresses $\sigma_a$ (stress along AD) and $\sigma_t$ (tangential stress). Plastic flow begins when the effective shear stresses $\sigma_{eg}$ reach the CRSS $\tau_0$ for that system. The calculation leads to a flow condition for each deformation system $n$:

$$\tau_{0n} = a_n\sigma_a + b_n\sigma_t \tag{1}$$

$a_n$ and $b_n$ can be calculated from the orientation relationship between the deformation system $n$ and the coordinate system given by the acting stresses.

The lack of data on the CRSS for single crystals can be overcome by normalizing all stresses to the CRSS ($=\tau_0$). In the case of prismatic slip ($\tau_0 = \tau_p$) one obtains from Eq. (1):

$$\frac{\sigma_a}{\tau_p} = \frac{b_m}{a_m}\frac{\sigma_t}{\tau_p} + \frac{1}{a_m} \tag{2}$$

Using the specific orientations of single crystals mentioned above results in Eq. (3):

$$\frac{\sigma_a}{\tau_p} = \cos^2\gamma\frac{\sigma_t}{\tau_p} \pm \frac{4}{\sqrt{3}} \tag{3}$$

The graph $\sigma_a/\tau_p = f(\sigma_t/\tau_p)$ gives straight parallel lines having slopes of $\cos^2\gamma$ and points of intersections with the $\sigma_a$-axis of $\pm 4 \cdot 3^{-1/2}$ respectively.

Regarding twinning systems the difficulty of normalizing can be solved by expressing the CRSS for twinning $\tau_i$ as a function of the CRSS for prismatic slip:

$$\tau_i = k_i \cdot \tau_p \tag{4}$$

$k_i$ is a specific constant for each twinning system $i$.

The combination of Eqs. (1) and (4) gives for the twinning system $i$

$$\frac{\sigma_a}{\tau_p} = -\frac{b_i}{a_i}\frac{\sigma_t}{\tau_p} + \frac{k_i}{a_i} \tag{5}$$

Eq. (5) means that the slope of the corresponding straight line is independent on $k_i = \tau_i/\tau_p$, while the points of intersection with $\sigma_a$-axis depend on the $k_i$-values.

Each deformation system is related to a straight line in the $\sigma_a/\tau_p - \sigma_t/\tau_p$ coordinate system, and the envelope of those straight lines is the yield locus (Dressler *et al.* 1973; Burggraf and Wincierz 1981).

Figure 4 shows the calculated yield loci for $\gamma = 0°$, 30°, 50° and 70° normalized for the CRSS of prismatic slip $\tau_p$. The onset of plastic flow in response to tensile stresses in the AD is in all cases determined by prismatic slip and does not depend on $\gamma$. The slope $m$ of the associated yield locus line is given by $\cos^2\gamma$ (see Eq. (3)). Different twin systems are activated in the first quadrant, depending on the tilt angle $\gamma$ of the basal pole. If the ratio of the CRSS is varied for prismatic slip and twinning, the yield loci of the twin

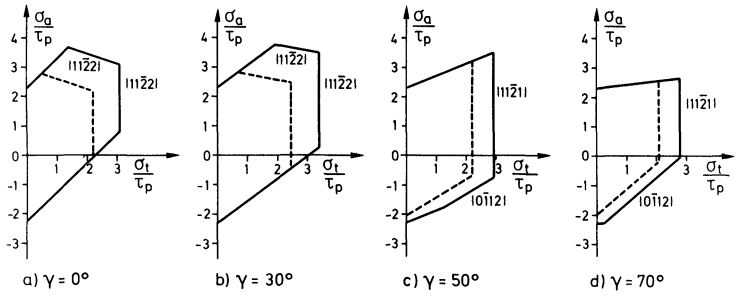


**Figure 4** Calculated yield loci for single crystals with [10$\bar{1}$0] parallel to the axial direction and different tilt angles $\gamma$. Stresses are normalized to the CRSS for prismatic slip $\tau_p$. Ratio of CRSS for {11$\bar{0}$0}-slip, {10$\bar{1}$2}-, {11$\bar{2}$1}- and {11$\bar{2}$2}-twinning = 1:1:1:1 (dashed lines) resp. = 1:1.25:1.35:1.4 (full lines).

systems undergo a parallel shift (Eq. (5)). This phenomemon was used to estimate the ratio of the CRSS by comparison with experimental yield loci leading to the ratios of CRSS for {1$\bar{1}$00}-slip, {10$\bar{1}$2}-, {11$\bar{2}$1}-, {11$\bar{2}$2}-twinning of 1:1.25:1.35:1.4 resp. (Dressler *et al.* 1972, 1973). For these ratios—which were used in Figure 4—the intersection with the positive $\sigma_t$-axis is defined by prismatic slip for tilt angles of the basal pole $\gamma = 0$ to 30°. The intersection of the axis $\sigma_t$, i.e. the onset of plastic flow caused by unaxial tangential tensile stress, increases as $\gamma$ increases.

Analogous results for the axis intercepts are obtained also for single crystals with [11$\bar{2}$0] parallel to the tube axis and $\gamma = 0$ to 30° (Figure 5). However, the form of the yield locus in the first quadrant is different from that of Figure 4. For single crystals with

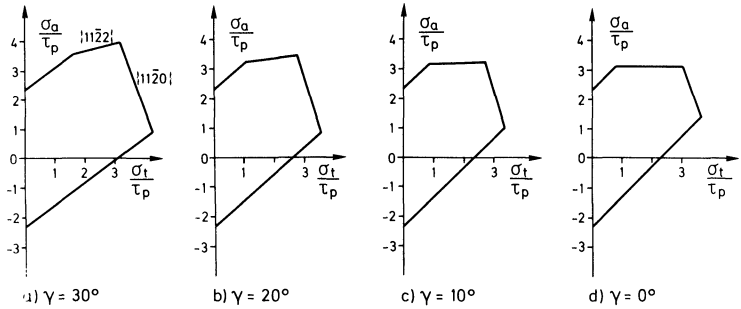


**Figure 5** Calculated yield loci for single crystals with [11$\bar{2}$0] parallel to the tube axis. Normalized as in Figure 4. Ratio of CRSS for {1$\bar{1}$00}-slip and {11$\bar{2}$2}-twinning 1:1.4.

[10$\bar{1}$0] parallel to the axial direction the onset of plastic flow under stress ratios $0 < \alpha < 1 (\alpha = \sigma_a/\sigma_t)$ is independent of additional axial stresses. However, the onset of plastic flow for single crystals with [11$\bar{2}$0] parallel to the tube axis depends on the additional axial stress (Figure 5). These qualitative differences were confirmed by comparing experimental yield loci for tubes with deformation textures and recrystallization textures (Matucha 1978).

## 2.2 Yield loci for polycrystals

Rather than describing the texture by one single crystal orientation, the analyses of the (0001)-pole figures is based on the distribution of basal poles in the plane formed by the RD and the TD, i.e. on the intensity profiles as shown in Figure 3. Each point $i$ on the profile curve is defined by the tilt angle $\gamma_i$ and the associated intensity $I_i$. The tilt angle $\gamma_i$ characterizes the single crystal orientation $i$, while $I_i$ describes its strength in units of random orientation.

Confining oneself at first to an investigation of those parts of the yield locus which are independent of twinning, the objective is to calculate $m_i$ for the crystals so defined and then to derive the slope $m_m$ for the tube with the respective texture. For each crystal $i$, the following relationship holds true:

$$m_i = \cos^2 \gamma_i \tag{6}$$

The contribution made by crystal $i$ to the total slope depends on $I_i$. Therefore, the values $\cos^2 \gamma_i$ have to be weighted with their respective intensities $I_i$:

$$I_i \cdot m_i = I_i \cos^2 \gamma_i \tag{7}$$

The average slope $m_m$ is obtained by integrating this equation over all $\gamma_i$ between $\gamma = -\pi/2$ and $\gamma = +\pi/2$:

$$m_m = \frac{\int_{\pi/2}^{+\pi/2} I(\gamma) \cos^2 \gamma \, d\gamma}{\int_{\pi/2}^{+\pi/2} I(\gamma) \, d\gamma} \tag{8}$$

For practical applications, it is more convenient to replace the integrals by sums and approximate the intensity curves by a step

function. A numerical evaluation is facilitated by subdividing the $\gamma$-range into $n$ identical intervals $\Delta\gamma$. It is then very easy to calculate $m_m$, i.e. the slope of the yield locus at the intersection with the $\sigma_a$-axis from the intensity profile.

An improvement of the calculation procedure to cover the entire yield locus, i.e. including also the segments dominated by twinning, is principally possible in the same way. This means that yield loci are calculated for single crystals defined by the tilt angles $\gamma_i$ and by $I_i$ on the basis of the respective intensity profiles and these yield loci are then considered in the averaging process according to their respective $I_i$.

## 3 COMPARISON OF CALCULATED VALUES WITH EXPERIMENTAL RESULTS

The calculation procedure is first used and the results are compared with experimental findings for the slope of the yield loci at the intersection with the positive $\sigma_a$-axis. This slope is independent of twinning (see above). For calculation purposes, the $\gamma$-area of the intensity profiles (see Figure 3) was subdivided into $\Delta\gamma$-intervals of 10°. Within these intervals an average was calculated for the corresponding intensity $I_i$. The slopes $m_m$ obtained by the procedure above were used to derive the slope angle $\beta_m$.

Data both from the literature and from own—in some cases still unpublished—experiments are used for comparison between calculated and measured slope angles in Table 2. The following conclusions can be drawn:

—If only a few single crystal orientations are used for calculation (column 2), the differences between calculated and measured values are in some cases considerable (see columns 3 and 5).

—If, on the other hand, the distribution of the orientation throughout the entire $\gamma$ area is considered, the experimental and calculated figures are in very good agreement (see columns 4 and 5).

If, as a second step, other points on the yield locus for tubes with deformation or recrystallization textures are calculated and compared with measured data, the results are those shown in Figures 6

**Table 2** Slope of the yield locus at the intersection point with the positive $\sigma_a$-axis. Comparison of measured and calculated values

| Material | $\gamma$ for single crystal replacement | Calculated slope angles from few single crystals | from intensity profiles RD–TD | Measured slope angles | Reference |
|---|---|---|---|---|---|
| Zircaloy-4, stress relieved | 0°, 30° | 36.9° | 32.5° | 27.5–32.5° | Dressler *et al.* 1973 |
| Zircaloy-4, stress relieved | 50° | 22.5° | 26° | 21° | Dressler *et al.* 1973 |
| Zircaloy-4, stress relieved | 70° | 6.7° | 21.8° | 21.2° | Dressler *et al.* 1972 |
| Zircaloy-4, recrystallized | 0°, 45° | 26.6° | 32.2° | 33–34.5° | Dressler *et al.* 1972 |
| Zircaloy-4, stress relieved | 0°, 35° | 33.9° | 32.1° | 27.5° | Dressler *et al.* 1972 |
| Zircaloy-4, stress relieved | 24° | 39.8° | 32.4° | 31.5° | Dressler *et al.* 1972 |
| Zircaloy-4, stress relieved | 0°, 45° | 26.6° | 29.9° | 28.5° | unpublished data |
| Zircaloy-4, stress relieved | 0°, 45° | 26.6° | 30.2° | 27° | unpublished data |
| Zircaloy-4, partly recryst. | 0°, 45° | 26.6° | 30.6° | 31° | unpublished data |
| Zircaloy-4, recrystallized | 0°, 45° | 26.6° | 31.8° | 28° | unpublished data |
| Zircaloy-2, stress relieved | 0°, 30° | 36.9° | 29.7° | 31° | Matucha 1978 |
| Zircaloy-2, stress relieved | 0°, 45° | 26.6° | 32.6° | 30° | Matucha 1978 |
| Zircaloy-2, partly recryst. | 0°, 45° | 26.6° | 31.6° | 31° | unpublished data |
| Zircaloy-2, partly recryst. | 0°, 45° | 26.6° | 33.1° | 32.5° | unpublished data |
| Zircaloy-2, recrystallized | 0°, 45° | 26.6° | 34.6° | 35° | Matucha 1978 |

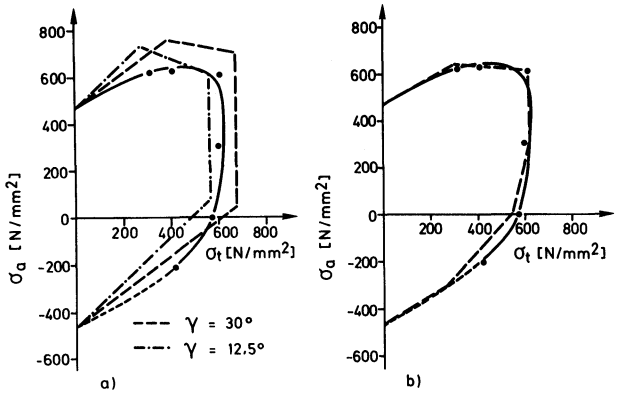


**Figure 6** Comparison of calculated and measured yield loci of Zircaloy-4, stress relieved. a) Measured points and yield locus (full line). Yield loci calculated for single crystal with $\gamma = 12.5°$ and $\gamma = 30°$. $[1\bar{1}00]$ parallel to AD. b) Dashed lines calculated using the distribution and intensity of basal poles.

and 7 for Zircaloy-4 cladding tubes. Calculations on the basis both of one or two single crystal orientations and of the basal pole distributions were made with the CRSS-ratios used so far. If the basal pole orientation distribution is considered (Figures 6b, 7b), this leads to a quantitative agreement between calculated and measured yield loci.

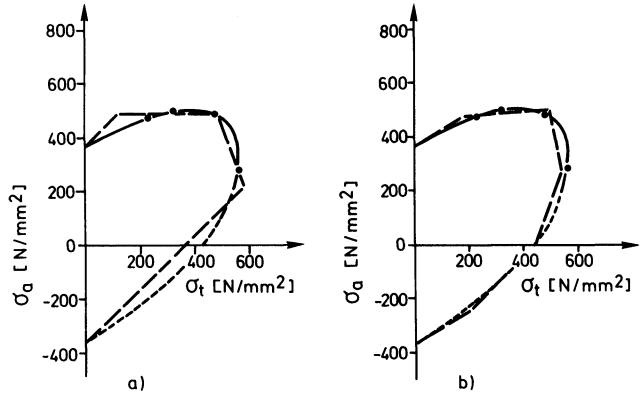


**Figure 7** Comparison of calculated and measured yield loci of Zircaloy-4, recrystallized. a) Dashed lines calculated yield locus for a single crystal with $\gamma = 0°$ and $[11\bar{2}0]$ parallel to AD. b) Dashed lines calculated using the distribution and intensity of basal poles.

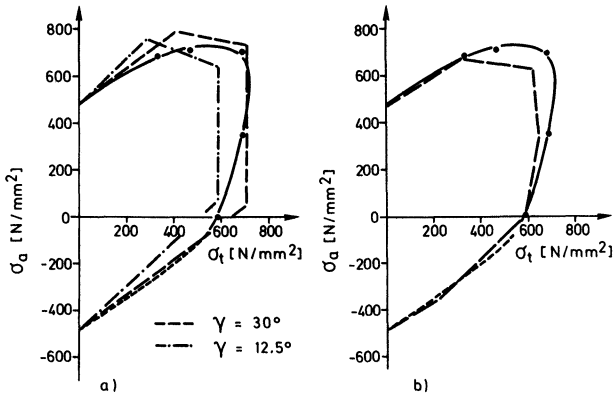


**Figure 8** Comparison of calculated and measured yield loci of Zircaloy-2, stress relieved. a) Measured points and yield locus (full line). Yield loci calculated for single crystal with $\gamma = 12.5°$ and $\gamma = 30°$. $[1\bar{1}00]$ parallel to AD. b) Dashed lines calculated using the distribution and intensity of basal poles.

For Zircaloy-2 cladding tubes (Figures 8 and 9), the measured and calculated data agree only for those points or areas which are determined by prismatic slip. In the case of points or areas defined by twinning, the calculated stresses are smaller for the onset of plastic flow if the CRSS-ratios for Zircaloy-4 are used.

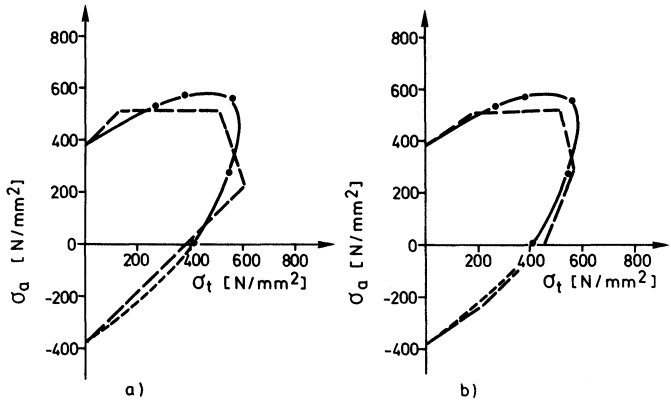


**Figure 9** Comparison of calculated and measured yield loci of Zircaloy-4, recrystallized. a) Dashed lines calculated yield locus for a single crystal with $\gamma = 0°$ and $[11\bar{2}0]$ parallel to AD. b) Dashed lines calculated using the distribution and intensity of basal poles.

## 4 EXPERIMENTAL EVIDENCE OF TWINNING

### 4.1 Investigations

Although mechanical twinning has generally to be expected when Zircaloy undergoes plastic deformation, twinning systems in biaxially loaded tubes could so far not be confirmed directly. The reason lies in the fact that past investigations concentrated on stress-relieved tubes of high dislocation densities. This made straight forward transmission electronmicroscopy observation more difficult. If twins were observed, nevertheless, it would have to be proved that they had not yet been present in the original condition, i.e. in the stress-relieved tube, but had formed during the measurements of yield loci. Such a verification is practically impossible. An attempt is therefore made hereunder at verifying mechanical twinning by way of changes in the texture.

The investigations refer to Zircaloy-2 tubes, whose recrystallization texture is shown in Figure 2. For a subsequent investigation, textures were determined from the tube samples, which had been exposed to plastic deformation in order to determine the yield loci. Quantitative (0001)- and $\{10\bar{1}0\}$-pole figures were established as described by Matucha (1978). The investigations were made after a uniaxial tensile test ($\sigma_a/\sigma_t = \infty$) and with $\alpha = 0$ (corresponding to a uniaxial tensile test in tangential direction).

These samples were selected because their plastic deformation was large in comparison with the samples tested under biaxial loads. They are therefore particularly suitable to measure changes in the texture. With $\alpha = \infty$ the elongation reached approx. 3.5% in axial direction, with $\alpha = 0$ it reached approx. 5.5% in the respective direction of stress.

### 4.2 Results

Figure 10 shows the (0001)- and $\{10\bar{1}0\}$-pole figures after plastic deformation in axial direction. In comparison with the texture prior to deformation (Figure 2), the $[10\bar{1}0]$ directions are now parallel to the tensile stress along the tube axis (Figure 10), whereas the distribution of basal poles has changed only slightly (Figure 10). If the tensile stress is applied tangentially to the tube, the intensities of

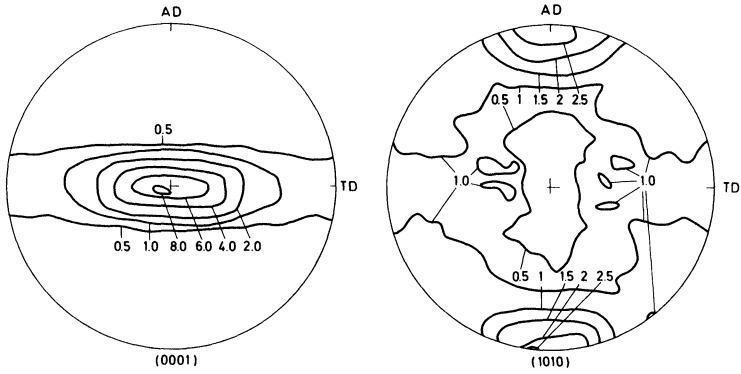


**Figure 10** Quantitative (0001)- and $\{10\bar{1}0\}$-pole figures of recrystallized Zircaloy-2 tube after plastic deformation under axial stresses.

the $\{10\bar{1}0\}$ poles (Figure 11) in the direction of the stress are also found to increase. However, the distribution of basal poles has changed fundamentally (Figure 11). Weak intensity maxima are measured in the plane described by the radial and axial directions. These maxima occur at an angle of approx. 65° from the radial direction.

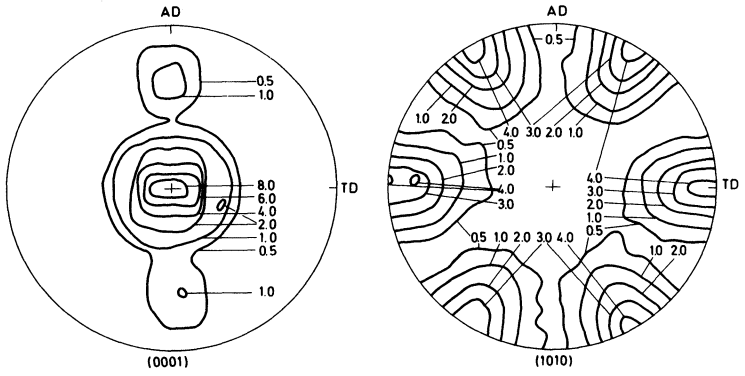


**Figure 11** Quantitative (0001)- and $\{10\bar{1}0\}$-pole figures of recrystallized Zircaloy-2 tube after plastic deformation under tangential stresses.

The change in the texture measured after a tensile stress had been applied axially can be explained by prismatic slip. On the other hand, the change in the distribution of basal poles after deformation with $\alpha = 0$ (Figure 11) indicates a spontaneous rotation of the lattice typical for twinning. Furthermore the angle of the new orientation (approx. 65° from the radial direction) is in good agreement with the angle 64.22° of rotation of basal poles by $\{11\bar{2}2\}$-twinning in Zirconium (Tenckhoff 1980, Ballinger *et al.* 1984).

## 5 DISCUSSION OF RESULTS

To calculate yield loci of polycrystalline Zircaloy on the basis of the Sachs model (Sachs 1928) the texture of cladding tubes can be better described in a simple way by the basal pole distribution in the plane formed by the radial and tangential directions, which can be easily gained from the pole figures.

The calculated slope of the yield loci at the intersection with the positive $\sigma_a$-axis depends—both for deformation textures and for recrystallization textures—only on the distribution of the basal poles and is independent of arbitrary assumptions about twinning. This slope is therefore particularly suitable for a comparison with measured values. This comparison leads to quantitative agreement.

A calculation of those areas of the yield locus which depend on twinning leads to good agreement with the values measured for Zircaloy-4 tubes, if the CRSS-ratios derived from previous investigations on Zircaloy-4 tubes are used. If the same ratios are used also for Zircaloy-2, the agreement with the measured values is not as good. The measured yield locus lies outside the calculated one. This might be explained by a higher CRSS for twinning than in the case of Zircaloy-4.

From the calculated yield loci it can be concluded that different twinning systems depending on the orientation and stress condition are activated (Dressler *et al.* 1973). Indirect confirmation of this conclusion could so far be obtained only from the asymmetry of the complete yield locus derived by experiments (Dressler *et al.* 1974) and from the qualitative agreement between calculated and measured yield loci (Dressler *et al.* 1972, 1973. Dressler and Matucha

1977, Matucha 1978). Although in this investigation the changes in texture were measured not for the onset of plastic flow but for relatively large elongations, the twinning system to be expected from the calculation may be regarded as confirmed.

The fact that the agreement between experimental and calculated results based on a rather simple texture replacement model is generally good allows the following conclusions as regards application:

The slope of the yield locus at the intersection with the positive $\sigma_a$-axis can be quantitatively calculated from the texture irrespective of twinning phenomena. As there is a direct relationship between this slope and the $R$-value (ratio of logarithmic diameter and logarithmic change in wall thickness), this value too can be calculated immediately from the texture.

Two measurements are required to predict the onset of plastic flow under biaxial stresses:

(1) The (0001)- and $\{10\bar{1}0\}$-pole figures make it possible to calculate the yield locus normalized to the unknown critical shear stress for prismatic slip.

(2) Measuring the axial yield stress, one obtains the intersection with the positive $\sigma_a$-axis to which the calculated yield locus can be fitted quantitatively.

## References

Althoff, J. and Wincierz, P. (1972). *Z. Metallkde* **63,** 623–633.
Althoff, J. (1973). *Aluminium* **49,** 799–802.
Ballinger, R. G., Lucas, G. E., Pelloux, R. M. (1984). *J. Nucl. Mat.* **126,** 53–69.
Burggraf, J. and Wincierz, P. (1981). *Z. Metallkde* **72,** 287–294.
Cuirchea, D. (1985). *J. Nucl. Mat.* **131,** 1–10.
Dressler, G., Matucha, K. H. and Wincierz, P. (1972). *Can. Met. Quart.* **11,** 177–184.
Dressler, G., Matucha, K. H. and Wincierz, P. (1973). Preprints of the 2nd Intern. Conf. on Structural Mechanics, in: *Reactor Technology,* Berlin, Vol. 1, C/2/2, 12 p.
Dressler, G., Drefahl, K. Matucha, K. H. and Wincierz, P. (1974), in: *Zirconium in Nuclear Application,* Spec. Techn. Publ. 551 (Am. Soc. Testing and Mater., Philadelphia, PA), 92–103.
Dressler, G. and Matucha, K. H. (1977), in: *Zirconium in the Nuclear Industry,* Spec. Techn. Publ. 633 (Am. Soc. Testing and Mater., Philadelphia, PA), 508–522.

Matucha, K. H. (1978), in: G. Gottstein, K. Lücke (Hrsg.), *Textures of Materials* (Springer, Berlin), Vol. II, 333–343.
Mehan, R. L. (1961). *Trans. ASME* **D83,** 499–512.
Miller, S. H. and Swota, J. (1963). *AEC Report* KAPL-2296.
Sachs, G. (1928). *Z. Verein. Deut. Ing.* **72,** 734–736.
Schmid, E. and Wassermann, G. (1928). *Z. Phys.* **48,** 370–383.
Schmid, E. and Wassermann, G. (1930). *Metallwirtsch.* **9,** 698–702.
Spiegelberg, P. and Anderson, Th. (1978), in: G. Gottstein, K. Lücke (Hrsg.), *Textures of Materials,* Springer, Berlin, Vol. II, 345–349.
Tenckhoff, E. (1980). *Verformungsmechanismen, Textur und Anisotropie in Zirkonium und Zircaloy,* Gebrüder Bornträger, Berlin, Stuttgart.
Tilch, W., Matucha, K. H. and Wincierz, P. (1982). *Z. Metallkde* **73,** 473–482.
Tomé, C. and Kocks, U. F. (1985). *Acta Met.* **33,** 603–621.
Wassermann, G. (1963). *Z. Metallkde* **54,** 61–65.
Wassermann, G. and Grewen, J. (1962). *Texturen metallischer Werkstoffe,* 2. Aufl. Springer Verlag Berlin, 554–669.